pH Dependence of the Photocycle Kinetics of the E46Q Mutant of Photoactive Yellow Protein: Protonation Equilibrium between I_1 and I_2 Intermediates, Chromophore Deprotonation by Hydroxyl Uptake, and Protonation Relaxation of the Dark State†

Berthold Borucki,‡ Harald Otto,‡ Chandra P. Joshi,‡ Chiara Gasperi,‡ Michael A. Cusanovich,§ Savitha Devanathan,§ Gordon Tollin,§ and Maarten P. Heyn*,‡

Biophysics Group, Department of Physics, Freie Universität Berlin, Arnimallee 14, D-14195 Berlin, Germany, and Department of Biochemistry and Molecular Biophysics, University of Arizona, Tucson, Arizona 85721

Received February 25, 2003; Revised Manuscript Received May 22, 2003

ABSTRACT: The kinetics of the photocycle of PYP and its mutants E46Q and E46A were investigated as a function of pH. E46 is the putative donor of the chromophore which becomes protonated in the I_2 intermediate. For E46Q we find that I_2 is in a pH-dependent equilibrium with its precursor I_1' with a pK_a of 8.15 and $n = 1$. From this result and from experiments with pH indicator dyes, we conclude that in the I_1' to I_2 transition one proton is taken up from the external medium. The pK_a of 8.15 is that of the surface-exposed chromophore in the equilibrium between I_1' and I_2 and is close to that of the phenolate group of *p*-hydroxycinnamic acid. The pH-dependent I_1'/I_2 equilibrium with associated H^+ uptake is reminiscent of the M_I/M_{II} equilibrium in the formation of the signaling state of rhodopsin. Well above this pK_a no I_2 is formed and I_1' returns in a pH-independent manner to the initial state P. The decay rate for the return to P via I_2 is between pH 4 and pH 8, exactly proportional to the hydroxide concentration (first order), and the deprotonation of the chromophore in this transition occurs by hydroxide uptake. Well above the pK_a of 8.15 the apparent rate constant for the return to P is constant due to the branching from I_1'. Complementary measurements with the pH indicator dye cresol red at pH 8.3 show that the remaining PYP molecules that still cycle via I_2 take up one proton in the formation of I_2. Together, these observations provide compelling evidence that during the photocycle the chromophore in E46Q is protonated and deprotonated from the external medium. For the yellow form of the mutant E46A the apparent rate constant for the return to P is also linear in [OH^-] below about pH 8.3 and constant above about pH 9.5, with a pK_a value of 8.8 for I_1', suggesting a similar mechanism of chromophore protonation/deprotonation as in E46Q. For wild type qualitatively similar observations were made: the amplitude of I_2 decreased at alkaline pH, I_1' and I_2 were in equilibrium, and I_1' decayed together with the return to P. Chromophore hydrolysis prevented, however, an accurate determination of the pK_a of I_1'. We estimate that its value is above 11. The ground state P is in the dark in a pH-dependent equilibrium with a low-pH bleached form P_{bl} with protonated chromophore. The pK_a values for these equilibria are 4.8 and 7.9 for E46Q and E46A, respectively. When the pH is close to these pK_a's, the kinetics of the photocycle contains additional components in the millisecond time range. Using pH-jump stopped-flow experiments, we show that these contributions are due to the relaxation of the P/P_{bl} equilibrium which is perturbed by the rapid decrease in the P concentration caused by the flash excitation of P. The condition for the occurrence of this effect is that the relaxation time of the P/P_{bl} equilibrium is faster than the photocycle time.

Photoactive yellow protein (PYP)[1] from the purple bacterium *Halorhodospira halophila* is a small water-soluble photoreceptor that is postulated to be involved in negative phototaxis (for recent reviews see refs *1* and *2*). PYP is the structural prototype for a large and diverse family of sensory and signaling proteins containing the PAS sequence motif (*1*, *3*, *4*). Its blue light absorption ($\lambda_{max} = 446$ nm) is due to a thioester-linked *p*-hydroxycinnamoyl chromophore. In the dark state P, the anionic form of the chromophore (*5*), is stabilized by hydrogen bonds to E46 and Y42 (*6*, *7*), and the 7−8 double bond of the chromophore is trans. Photoexcitation is followed by rapid isomerization around this bond (*8*, *9*) and a subsequent photocycle consisting of a number of spectrally distinguishable photointermediates (*10*, *11*). About 3 ns after photoexcitation, the red-shifted intermediate

† This research was supported in part by Grant Sfb 498-TP B1 from the Deutsche Forschungs Gemeinschaft to M.P.H. and NIH Grant GM66146 to M.A.C.

* To whom correspondence should be addressed: e-mail, heyn@physik.fu-berlin.de; phone, ++49-30-838 56160; fax, ++49-30-838 56299.

‡ Freie Universität Berlin.

§ University of Arizona.

[1] Abbreviations: PYP, photoactive yellow protein; FTIR, Fourier transform infrared; SVD, singular value decomposition; PAS, acronym formed from the names of the first three proteins of this family (*p*eriod clock protein, *a*ryl hydrocarbon receptor nuclear translocator, single-minded protein).

10.1021/bi034315d CCC: $25.00
Published on Web 07/01/2003

I_1 is formed ($\lambda_{max} = 465$ nm, decay time $\tau_D \approx 200$ μs) in which the hydrogen bond with E46 is still intact (*12*, *13*). In the following blue-shifted intermediate I_2 ($\lambda_{max} = 355$ nm, decay time $\tau_D \approx 2$ ms), this hydrogen bond is broken, and the phenolate moiety has rotated out of its initial binding pocket, exposing its oxygen to the solvent (*14*). In I_2 the chromophore is protonated (*9*, *15*), leading to the large spectral blue shift. One proton is taken up from the aqueous medium in the I_1 to I_2 transition, suggesting that the chromophore is protonated in this way (*17*). Recent time-resolved FTIR (*13*, *16*) and dye binding (*17*, *18*) studies showed that about 2 ms after flash excitation I_2 decays to another blue-shifted intermediate with a protonated chromophore, I_2' (decay time $\tau_D \approx 200$ ms). This transition is associated with a major conformational change of the protein as indicated by structural and spectroscopic methods in solution [NMR (*19*), FTIR (*16*), SAXS (*20*, *21*), and CD (*20*, *22*)]. The global structural change from I_2 to I_2' has also been described as a partial unfolding (*23*). The dyes bromocresol purple (*17*) and Nile red (*18*) bind transiently to the surface of the structurally altered I_2' intermediate. It is likely that the long-living I_2' intermediate rather than I_2 is the activated or signaling state in which PYP interacts with a response regulator that has not been identified to date. No large conformational change in I_2 was detected, however, in crystals by X-ray diffraction (*14*), with the main structural change limited to the chromophore and the binding pocket. In I_2 the chromophore reorients by about 60°, bringing its oxygen close to the protein surface (*14*). It is likely that in crystals packing constraints prevent the formation of I_2' and that the crystal structure of ref *14* refers to I_2.

An essential step in the formation of the signaling state (I_2 or I_2') is the protonation of the chromophore. One of the open questions is whether the chromophore is protonated by intramolecular proton transfer from E46 or by the aqueous medium after motion and exposure of the chromophore oxygen to the protein surface (*16*, *17*). Due to its very high pK_a no proton transfer is expected to occur from Q46 to the chromophore in the mutant E46Q. Yet the formation of the I_2 intermediate was considerably faster in E46Q than in wild type [110 vs 500 μs for wild type at pH 6.2 (*17*)]. Moreover, at pH 6.2 the formation of I_2 was exactly synchronized with the uptake of one proton from the aqueous medium, as determined by time-resolved absorption spectroscopy with the pH indicator dye bromocresol purple (*17*). These data strongly suggest that, in E46Q, the chromophore is protonated from the external medium (*17*).

It has been shown that the pH dependence of the kinetics of the formation and decay of I_2 differs substantially in E46Q and wild type (*7*). Although the time resolution was insufficient to resolve the rise of I_2 at high pH, data were collected for the decay of I_2 which indicated that the decay rate of I_2 accelerates about 700-fold from pH 5 to pH 9.5 (*7*). A pH plot of this rate constant had a sigmoidal shape with a pK_a of 8.0. In contrast with wild-type PYP the pH dependence was bell-shaped with the maximum at pH 8 and a maximal change in rate constant with pH of only 16-fold (*7*). The ionizable group responsible for the pK_a of 8.0 in E46Q has not been assigned. In this work we will show that this is the pK_a of the solvent-exposed chromophore in the equilibrium between the I_1' and I_2 intermediates with I_1' an intermediate between I_1 and I_2 with deprotonated chromophore in which the phenolic oxygen is exposed at the surface.

In another photocycle study on E46Q, complete spectra were recorded from 250 to 500 nm with a time resolution of 2 ms (*24*). At room temperature and pH 7.3, the decay of I_2 was found to be monoexponential with a time constant of 53 ms. The absorption maximum of I_2 was at 368 nm, i.e., red shifted by 11 nm with respect to wild type (*24*). On the basis of this observation, it was concluded that the chromophore remains hydrogen-bonded to Q46 in I_2 (*24*).

Here we present data on the pH dependence of the photocycle kinetics at 16 wavelengths covering the spectral bandwidths of the I_1, I_2, and P states with a time resolution of about 100 ns. These data are of sufficient signal to noise ratio (in particular in the UV) and time resolution to resolve the formation of I_2 directly at 370 nm. We find that the absorbance change at 370 nm due to I_2 goes to zero at high pH with a pK_a of 8.1. Moreover, we show that the logarithm of the decay rate of I_2 increases linearly with pH from 4 to 8 and levels off above pH 8. These data can be interpreted on the basis of a model with a pH-dependent equilibrium between I_1' and I_2, branching from I_1' directly to the dark state P and OH^- uptake in the decay of I_2. The pK_a of 8.1 represents the pK_a of the chromophore in the equilibrium between the I_1' and I_2 intermediates in which the chromophore is surface-exposed. Taken together, these data provide conclusive evidence for chromophore protonation from the aqueous medium.

In the dark, the yellow form of PYP is in a pH-dependent equilibrium with a bleached form, P_{bl}, with protonated chromophore absorbing around 350 nm (*25*, *26*). For wild type, the pK_a for this transition is at 2.8, for E46Q it is at 4.8, and for E46A it is at 7.9 (*27*). For wild type, this is the pK_a for acid denaturation with simultaneous protonation of the chromophore (*33*). For E46Q and E46A, the pK_a values refer to chromophore protonation in a native protein conformation. Here we show for E46Q and E46A that, when the pH is near the pK_a and, consequently, the fraction of molecules in the P_{bl} form considerable, the photocycle kinetics contain substantial contributions from the relaxation of this equilibrium on the millisecond time scale. In the past similar transient absorbance changes were observed for E46A but mistakenly attributed to transitions between photocycle intermediates (*17*, *27*).

MATERIALS AND METHODS

Sample Preparation. Native PYP from *H. halophila* and the mutants E46Q and E46A were prepared as described (*7*, *27*).

Transient Absorption Spectroscopy. Absorbance changes after flash excitation were recorded from ~100 ns to 50 s as described (*28*, *29*). The analysis of the kinetic data with SVD and global fitting was performed as described (*28*). The kinetics of proton uptake and release and the proton stoichiometry were measured as described (*17*, *28*, *30*). For these purposes, the pH indicator dye cresol red (p$K_a = 8.2$) was used at pH 8.3.

Stopped-Flow Measurements. The detection part of this apparatus was home-built. It consisted of a Xe light source, fiberoptic light guides to and from the mixing chamber, a 125 mm spectrometer (77400-M, Oriel Corp.), and a linear

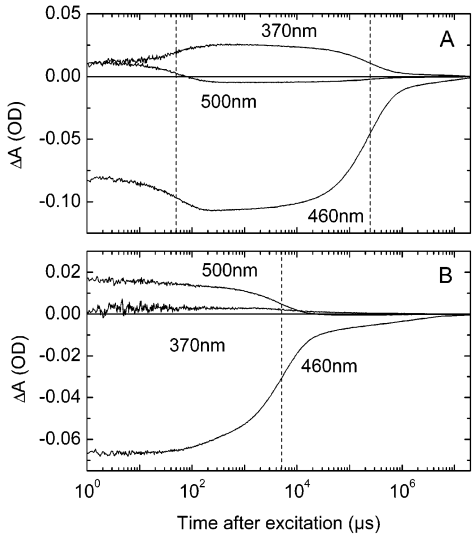

FIGURE 1: Transient absorbance changes $\Delta A(t)$ of the PYP mutant E46Q at the three wavelengths indicated. Panels: (A) pH 6.53; (B) pH 9.70. The dashed vertical lines mark the time constants of the main components in the rise and decay of I_2 (A) and in the recovery of P (B), respectively. Conditions: 20 mM Tris buffer, 50 mM KCl, 20 °C.

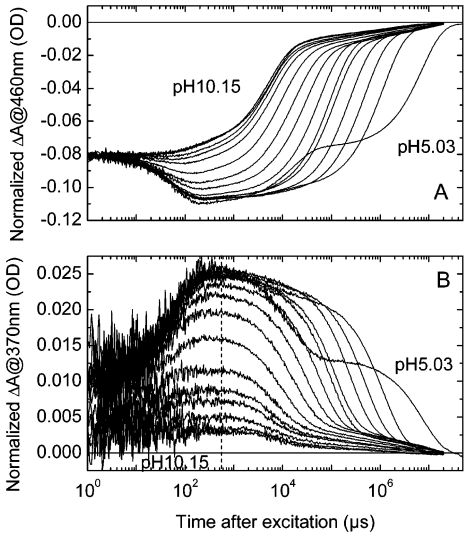

FIGURE 2: pH dependence of the transient absorbance changes of E46Q at 460 nm (A) and 370 nm (B). From right to left the pH values for the various time traces were 5.03, 5.81, 6.19, 6.53, 6.86, 6.96, 7.29, 7.56, 7.86, 8.20, 8.46, 8.76, 8.96, 9.33, 9.70, and 10.15. The dashed vertical line in (B) marks the time at which the amplitude of the 370 nm signal was read off. Conditions as in Figure 1.

CCD detection array (CCD2010, Entwicklungsbuero G. Stresing, Berlin, Germany) covering 512 wavelength points. Complete spectra were taken at 20000 discrete time points after mixing. The mixing unit (SHU-61) was from Hi-Tech (Salisbury, U.K.) and had a dead time of less than 2 ms. For the pH jump from 6.3 to 4.8, the mutant was initially suspended in 5 mM MES buffer at pH 6.3. After 1:1 mixing with 100 mM MES, pH 4.1, the final measured pH was 4.8.

RESULTS

pH-Dependent Equilibrium of I_1' to I_2. Figure 1 shows time traces at pH 6.53 (panel A) and pH 9.70 (panel B) of the transient absorption changes of the mutant E46Q at the wavelengths 460, 500, and 370 nm. These wavelengths are characteristic for the ground state depletion (negative absorbance change at 460 nm), for the transient occurrence of the red-shifted I_1 intermediate (positive absorbance at 500 nm), and for the strongly blue-shifted I_2 intermediate (positive absorbance at 370 nm). The latter blue shift is mainly due to the protonation of the chromophore in the I_1 to I_2 transition. From panel A we conclude that at pH 6.53 I_1 decays to I_2 with a time constant of about 50 μs (decay of absorbance at 500 nm and simultaneous rise of absorbance at 370 nm). This time constant is also clearly observable in the depletion signal, since I_1 has substantial absorbance at 460 nm. The dashed vertical line around 50 μs marks the common time constant for the I_1 to I_2 transition in these three time traces. The return of I_2 to the initial state P occurs with a time constant of about 250 ms at pH 6.53 (marked by the dashed vertical line). We note that the kinetics differ somewhat from those previously reported (*17*). This difference is due to the different conditions used here (20 mM Tris, 50 mM KCl) and in ref *17* (no buffer). The buffer affects the intermediate spectra. Panel B shows that at pH 9.70 the photocycle kinetics are very different. No absorbance increase occurs at 370 nm. The positive signal at 500 nm due to I_1 persists and decays together with the return to the initial state in the depletion signal, as indicated by the vertical line. These data show that at pH 9.70 no I_2 intermediate is formed. In agreement with this conclusion there is no contribution due to the I_1 to I_2 transition in the depletion signal; the absorbance change at 460 nm is flat from 1 to 100 μs. The photocycle kinetics were measured at 16 wavelengths (360−510 nm) from pH 4.4 to pH 10.25. The pH dependence at 460 nm is shown in Figure 2A from pH 5.03 to pH 10.15. In this figure the time traces at various pH values have been scaled in such a way that the level at 1 μs, due to I_1, is the same in all traces. This procedure is justified since the amount of PYP cycling is pH-dependent. In this way we normalize the traces at various pH values to the same amount of I_1. It is clear from Figure 2A that the amplitude of the I_1 to I_2 transition around 50 μs vanishes with increasing pH, as was already apparent from a comparison between panels A and B of Figure 1. The data show that the time constant for this transition is only weakly pH-dependent. Likewise, the amplitude of the I_2 signal at 370 nm vanishes at high pH (Figures 1B and 2B). In Figure 2B the time traces at 370 nm are shown from pH 5.03 to pH 10.15. The pH-dependent amplitude of the signal was evaluated at 550 μs. This time is marked by the vertical line in Figure 2B. In Figure 3A these two absorbance amplitudes are plotted against the pH and fitted simultaneously with a Henderson−Hasselbalch curve with $n = 1$ and $pK_a = 8.15 \pm 0.04$. Both the 370 and 460 nm contributions due to I_2 disappear with this pK_a. Separate fits to each data set lead to only slightly different values: $pK_a = 8.32$ and $n = 1$ at 370 nm; $pK_a = 8.07$ and $n = 1$ at 460 nm. With a different sample an independent data set was collected, leading to $pK_a = 8.14$ and $n = 1$. The fit is excellent. An initial interpretation of these results would be to assume a pH-dependent equilibrium between I_1 and I_2 with proton uptake by the chromophore and a pK_a of 8.15. Above this pK no I_2 is formed and I_1 decays directly to P. Thus there is branching at I_1. Let $k_{12}[H^+]$ be the forward rate from I_1 to I_2 and k_{21} the backward rate from I_2 to I_1. The apparent rate constant for the relaxation of this I_1/I_2 equilibrium would then be $k_{12}[H^+] + k_{21}$ and expected to be

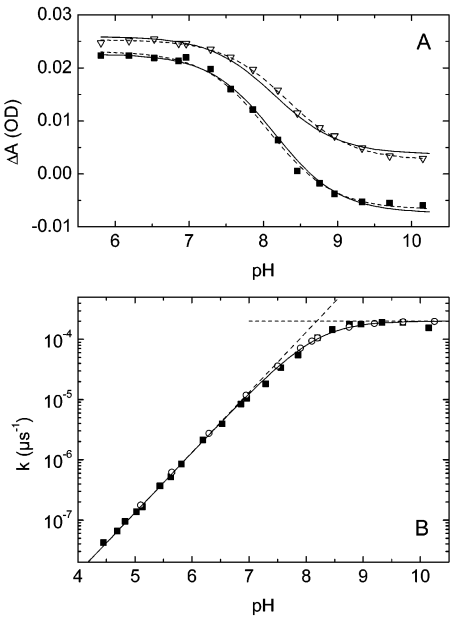

FIGURE 3: Analysis of the amplitudes and rate constants of the time traces of Figure 2 for E46Q. (A) pH dependence of the amplitude of the I_2 contribution in the depletion signal (■, 460 nm) and in the absorbance change at 370 nm (▽). The continuous curve is a simultaneous fit of both sets of titration data to the Henderson−Hasselbalch equation with pK_a = 8.15 ± 0.04 and n = 1.0. The dashed curves are the fits to each titration curve separately with pK_a = 8.32 for ▽ and pK_a = 8.07 for ■. (B) pH dependence of the rate constant (■, ○) of the major component in the recovery of P as obtained from the depletion signal at 460 nm. The data points labeled by ■ and ○ were obtained from two independent experiments with different samples. log k is plotted against pH. The continuous curve is a fit using eq 3 with pK_a = 8.18 ± 0.02. The dashed straight line with slope of +1 is the linear approximation based on eq 5. The dashed horizontal line is given by eq 4.

pH-dependent. We noted, however, from Figure 2A that the rate constant for I_1 to I_2 is only very weakly pH-dependent. We therefore need to postulate the following modified model:

$$I_1 \xrightarrow[k]{} I_1' \underset{k_{12}[H^+]}{\overset{k_{21}}{\longleftrightarrow}} I_2 \qquad (1)$$

In I_1 the phenolate of the chromophore is still buried and hydrogen bonded, presumably to Q46 and Y42. In the I_1 to I_1' transition the phenolate moves out to the surface. This is the rate-limiting step, and this chromophore reorientation is pH-independent. Once at the surface in I_1', the phenolate is rapidly protonated by the solvent. This model explains our observations for the kinetics of the rise of I_2, with pK_a = log k_{12}/k_{21}. The pK_a of 8.15 is thus interpreted as the pK for chromophore protonation in the equilibrium between the intermediate I_1' with surface-exposed chromophore and I_2.

Hydroxyl Uptake in the I_2 to P Transition. Another striking result from Figure 2 is the very strong pH dependence of the rate constant for the return from I_2 to the ground state below pH 8. Above pH 8, when no I_2 is formed, this rate (now from I_1') is no longer pH-dependent. This is to be expected since no chromophore protonation occurs. The data of Figure 2A show that at pH 5.03 a new feature develops in the kinetics: an additional faster component occurs around 10 ms in the depletion signal. This effect is also observed in the 370 nm signal (Figure 2B). The amplitude of this 10 ms component is strongly pH-dependent and starts to become significant below pH 5.8. The time traces between pH 5.81 and pH 4.24 are presented separately in Figure 6A. This fast 10 ms component will be discussed in more detail below and is, as we will show, unrelated to the deprotonation of the chromophore in the decay of I_2. Here we will focus on the slowest main component in the return of the depletion signal (Figures 2A and 6A). In Figure 3B the logarithm of this rate constant is plotted versus the pH. Over almost four decades, from pH 4.45 to pH 8, this pH dependence can be represented very well by the simple linear relationship log k = pH + constant with a slope of +1. This is equivalent to $k \sim [OH^-]$ and means that the reaction is first order in the hydroxide concentration and specific base catalyzed (*38*, *39*). Above pH 8.5 this rate constant is pH-independent. To explain our results, the model of the previous section needs to be expanded as follows to include the decay of I_2:

$$I_1 \xrightarrow[k]{} I_1' \underset{k_{12}[H^+]}{\overset{k_{21}}{\longleftrightarrow}} I_2 \xrightarrow[k_3[OH^-]]{} P; \quad I_1' \xrightarrow[k_4]{} P \qquad (2)$$

Since the decay rate of I_2 is first order in the hydroxide concentration, the chromophore deprotonates by OH^- uptake rather than by H^+ release. The release of protons (dissociation reaction) would be expected to be pH-independent. OH^- uptake provides the only mechanism to explain the data. We note that the dye signal associated with this transition has been interpreted as proton release (*17*). On the basis of the pH dye signals, one cannot distinguish between these two possibilities. We assume, moreover, that the I_1'/I_2 equilibration is fast, also compared to the decay of I_2. The apparent rate constant for the recovery of P is then given by

$$k_{app} = \frac{k_3 \times 10^{pK-14} + k_4}{10^{pK-pH} + 1} \qquad (3)$$

with $k_{21}/k_{12} = 10^{-pK}$. The limiting behavior of eq 3 above and below the pK should be in accordance with our observations. For pH ≫ pK, k_{app} approaches the constant limiting value

$$k_{app}^{\infty} = k_3 \times 10^{pK-14} + k_4 \qquad (4)$$

The superscript ∞ refers to the limit of infinite pH. When pH ≪ pK, k_{app} is given by $(10^{pH-pK})k_{app}^{\infty}$. At pH values below the pK we thus have the observed linear relationship

$$\log k_{app} = pH - pK + \log k_{app}^{\infty} \qquad (5)$$

This linear approximation to eq 3 is represented in Figure 3B by the straight dashed line of slope +1. The fit according to the full equation (eq 3) is also shown in Figure 3B (solid line). This fit required a pK_a of 8.18 ± 0.02. This value can also be taken directly from Figure 3B, since the intersection of the straight lines according to eqs 5 and 4 occurs at the pK_a. The second fit parameter was $k_{app}^{\infty} = 2.01 \times 10^2$ s^{-1}. The excellent fit to eq 3 based on the simple model (eq 2) over the entire pH range shows that this model provides an adequate description of the observed extreme pH dependence. Again the pK_a of 8.18 represents the pK of the chromophore in the I_1'/I_2 equilibrium when exposed to the solvent. Above this pK the chromophore can no longer be protonated, no I_2

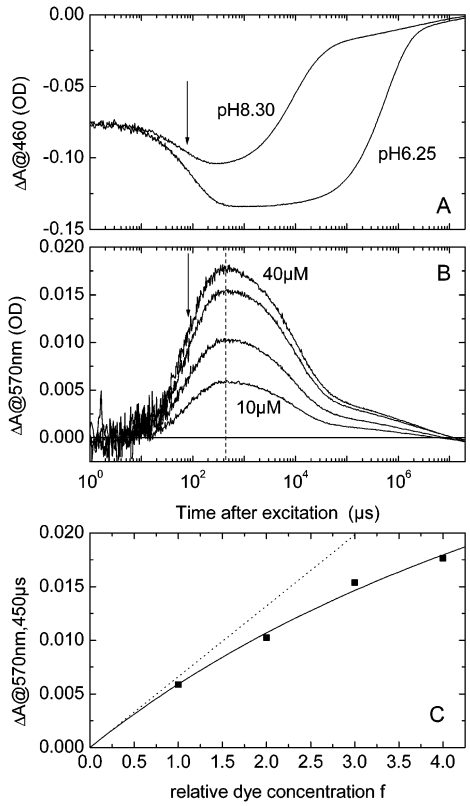

FIGURE 4: Kinetics and stoichiometry of proton uptake by E46Q at pH 8.30 in the absence of buffer. (A) Time traces of the depletion signal (460 nm) at pH 6.25 and pH 8.30, normalized at 1 μs. (B) Light-induced transient absorption changes at 570 nm of E46Q (concentration 10 μM, pH 8.30) at four different concentrations of the pH indicator dye cresol red (10, 20, 30, 40 μM). The dashed vertical line is at 450 μs. The arrows in (A) and (B) indicate the common time constant for the rise of I_2 and the proton uptake. (C) Dye signal at 450 μs (solid squares) versus relative dye concentration f = [dye]/10 μM. The solid line is a fit to the data with eq 1 of ref *17*. The dotted line indicates the predicted dependence in the absence of saturation effects.

is formed, and I_1' decays directly to P with the pH-independent rate k_4.

Proton Uptake Stoichiometry in I_2 Formation. As a further test of the model, we measured the kinetics and the stoichiometry of proton uptake using the pH indicator dye cresol red (pK_a = 8.2). We selected this dye because it allows measurements of transient proton uptake at pH 8.3, i.e., in the range of the pK_a of 8.15−8.18 for the I_1'/I_2 equilibrium. Such measurements have to be performed in the absence of buffer. Figure 4A shows the time traces for the depletion signal of an unbuffered sample of E46Q at pH 6.25 and 8.30. As expected, the amplitude of the contribution due to the I_1 to I_2 transition at pH 8.30 is also, in the absence of buffer, much reduced compared to its value at pH 6.25; i.e., at pH 8.30 the I_1'/I_2 equilibrium is on the side of I_1'. Figure 4B shows the dye signal at 570 nm at a protein concentration of 10 μM at various dye concentrations. The proton uptake kinetics at pH 8.30 are perfectly synchronized with the I_1 to I_2 transition in the depletion signal (compare arrows in Figure 4A,B), as it should be according to our model. Of particular interest at pH 8.3, where more than half of the molecules decay directly from I_1' to P without proton uptake, is the H^+ stoichiometry. This is determined from the fit of the amplitude of the dye signal at various dye concentrations according to the procedure developed in ref *17*. The data and the fit are shown in Figure 4C. To calculate the proton stoichiometry, we need the concentration of E46Q molecules cycling. Because of the branching at I_1' and the assumption of our model that protons are only taken up in the pathway via I_2, the I_2 concentration must be used. As shown in Figure 4A at pH 8.30 the I_2 concentration is less than half that at pH 6.25. Thus by defining the stoichiometry as protons taken up per I_2 molecule, we obtain in Figure 4C a value of 1.0 ± 0.4. In our previous study (*17*) we obtained 1.2 ± 0.2 at pH 6.3. Had we used the concentration of I_1 in the definition of the stoichiometry, we would have obtained a number of less than 0.5. We conclude that the apparent stoichiometry decreases with increasing pH from 6.3 to 8.3 when we normalize to the concentration of I_1 but remains around 1 when we normalize to the concentration of I_2 formed. Thus, those few E46Q molecules that still return to P via I_2 at pH 8.30 take up one proton as at pH 6.3. The experimental value of 1 for the proton stoichiometry is thus in good agreement with the model (eq 2) and supports the pH-dependent branching at I_1'. A stoichiometry of near 1 was also obtained by reducing the protein concentration to 1 μM, where nearly every proton taken up is detected by the excess (40 μM) dye molecules (saturation).

We note that the dye signal contains a small, very slowly decaying component (Figure 4B), which can also be observed in the corresponding depletion signal as well as in the 370 nm signal at high pH (Figure 2B). The decay of this component is nonexponential, is not due to a diffusional artifact in the flash photolysis experiment, and is not a light scattering background from aggregates. At present we have no explanation except that it might be due to a minority population with a different photocycle. Due to this long tail the time traces of Figure 2A could not be fitted satisfactorily by a sum of exponentials. For this reason the rate constants for the main early decay component derived from the data of Figure 2A and represented in Figure 3B were obtained from the points of inflection of the time traces. For a single exponential this method provides an accurate method of determining the exponential rate constant.

Wild-Type Photocycle at Alkaline pH. To explore the relevance of these observations with E46Q for wild type, we measured the wild-type photocycle kinetics above pH 10. Usually photocycle measurements are limited to the pH range below 10 because of the slow hydrolysis of the chromophore above pH 10. However, the 10 transient time traces required for a reasonable signal to noise ratio can be obtained quickly. Moreover, a fresh aliquot can be used for every high-pH point, and the amount of hydrolysis can be determined by photocycle measurements at pH 7 after measurement at high pH (reversibility) and by the absorption spectra. Figure 5 shows the time traces at 370 and 490 nm for wild-type PYP, indicative for the concentrations of the I_2 and I_1 intermediates, respectively, at pH 7.94 (A) and pH 10.94 (B). These data clearly show that, around pH 11, the ratio of the amplitudes at 370 and 490 nm is reduced compared to the ratio at pH 7.9. Moreover, in the millisecond to second range, the signal at 490 nm remains positive and decays together with the recovery of P. Additional data at intermediate pH values (not shown) demonstrate that, with increasing pH, the concentration of I_1 increases at the expense of I_2 and that I_1 and I_2 coexist after the rise of I_2. Figure 5B shows that, at pH 11, I_2 and I_1 are in equilibrium just as in

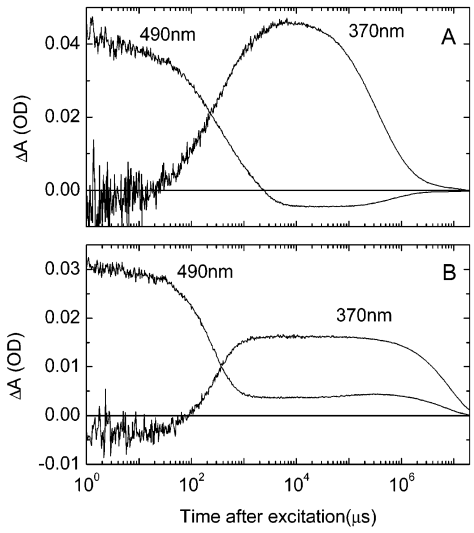

FIGURE 5: Transient absorbance changes $\Delta A(t)$ of wild-type PYP at 370 and 490 nm at pH 7.94 (A) and 10.94 (B). Conditions: 5 mM Tris buffer, 20 °C.

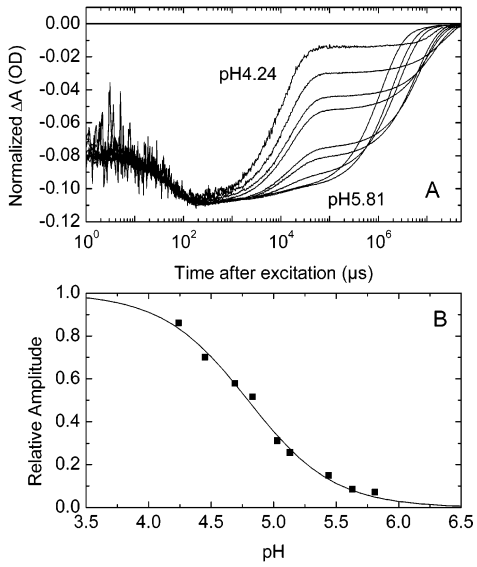

FIGURE 6: pH dependence of the transient absorbance change of E46Q at 460 nm in the neighborhood of the pK_a of 4.8 for the dark equilibrium P/P_{bl}. (A) Time traces from pH 5.81 to pH 4.24 normalized at 1 μs. From top to bottom the pH values for the various time traces were 4.24, 4.45, 4.69, 4.83, 5.03, 5.13, 5.44, 5.63, and 5.81. (B) pH dependence of the relative amplitude of the 10 ms component in the decay of I_2 (■). The data in (B) were fitted using the Henderson−Hasselbalch equation with pK_a = 4.80 ± 0.02 and n = 1.27 ± 0.07.

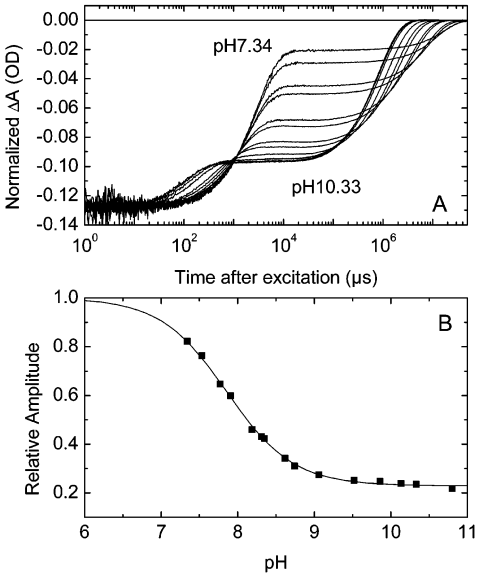

FIGURE 7: pH dependence of the transient absorbance change of E46A at 470 nm in the neighborhood of the pK_a of 7.9 for the dark equilibrium P/P_{bl}. (A) Time traces from pH 7.34 to pH 10.33 normalized at 100 ns. From top to bottom the pH values for the various traces are 7.34, 7.53, 7.77, 7.91, 8.35, 8.62, 8.74, 9.06, 9.52, 9.68, 10.13, and 10.33 (B) pH dependence of the relative amplitude of the 10 ms component in the decay of I_2 (■). The data in (B) were fitted using the Henderson−Hasselbalch equation with pK_a = 7.86 ± 0.02 and n = 1 (fixed). Conditions: 20 mM Tris buffer, 50 mM KCl, 20 °C.

E46Q near the pK_a of 8.15. The amplitude of the I_1 to I_2 transition in the depletion signal also decreased at pH 11. Thus the pH dependence in wild type above pH 10 is qualitatively similar to that of E46Q above pH 7. Short periods of time at pH 10.94 resulted in no loss of chromophore and titration back to pH 7.0 led to the same photocycle kinetics. However, above pH 11, irreversible effects occurred, and no meaningful data could be collected. It was thus not possible to determine an apparent pK_a for this transition in wild type, but it is clearly above 11.

Relaxation of P/P_{bl} Equilibrium Contributes to Photocycle Kinetics. We noted that at pH 5.03 an additional 10 ms component contributed to the decay of the depletion signal in Figure 2. We observed a similar millisecond component with the E46A mutant at pH 8.3 in the depletion signal at 370 nm (I_2) and in the pH indicator signal (*17*). The nature of this transition, which apparently involves proton release and I_2 decay, remains obscure. For wild type, the yellow form P is in equilibrium in the dark with a bleached blue-shifted form P_{bl} with a protonated chromophore absorbing around 350 nm. For wild type, the pK_a for this equilibrium is at 2.8, and for E46Q and E46A the corresponding pK_a's are at 4.8 (*33*) and 7.9 (*27*), respectively. In Figure 6A the pH dependence of the depletion signal is shown for E46Q from pH 5.81 to pH 4.24, i.e., in the neighborhood of the pK_a of 4.8. It was observed that the signal level due to I_1 decreases with decreasing pH and that the relative amplitude of the 10 ms component increases with decreasing pH. The decrease in the amplitude of the depletion signal at 1 μs with decreasing pH is simply due to the decreased amount of PYP molecules cycling since the dark equilibrium is shifted in the direction of P_{bl}. The time traces in Figure 6A were therefore again normalized at 1 μs, i.e., to the same amount of I_1. The data in Figure 6A were fitted with a sum of three exponentials. The first component with amplitude A_1 and a time constant of about 50 μs is pH-independent. The amplitude A_2 of the second component with time constants varying between 10 and 15 ms is the one of interest. The third component with amplitude A_3 has a time constant varying between 1 and 30 s. In Figure 6B the relative amplitude of this 10 ms component $[A_2/(A_2 + A_3)]$ is plotted versus pH and fitted to a Henderson−Hasselbalch curve with n = 1.27 ± 0.07 and pK_a = 4.80 ± 0.02. Corresponding data for E46A at pH values in the neighborhood of its pK_a are shown in Figure 7. In contrast to E46Q the amplitude of the millisecond relaxation component does not vanish completely at high pH. We note that the very fast formation of I_2 with approximately 2 μs (*17*) is not resolved in Figure

7A. This is due to the fact that the analogue bandwidth of the amplifier was set to 1 MHz in order to obtain an adequate signal to noise ratio in the time range above 10 μs. The results of the data analysis are shown in Figure 7B. The relative amplitude of the A_2 component in Figure 7B was fitted with a pK_a of 7.86 $\pm$ 0.02 and $n = 1$ (fixed). The excellent agreement of the pK_a values determined in this way from the photocycle with those obtained from the titration in the dark suggests that this millisecond component is indeed associated with the dark equilibrium between the yellow state at 460 nm (470 nm for E46A, respectively) and the bleached form at 350 nm. We note that additional data on the low-pH side would have been desirable in Figures 6B and 7B. However, below the pK_a values for the P/P_{bl} equilibrium, almost no P remains and photocycle data of sufficient signal to noise ratio could not be collected. Our observations may be explained as follows. With decreasing pH in the neighborhood of the pK_a (4.8 for E46Q and 7.9 for E46A) the concentration of the yellow form in the dark decreases and leads to a corresponding decrease in the number of molecules entering the photocycle as expressed by the stationary amount representing I_1 at around 100 ns. Flash excitation leads to a concentration jump (decrease) in P. If the transition between I_2 and P is slower than the relaxation between P_{bl} and P, the reequilibration between these two forms will occur during the photocycle with a conversion from P_{bl} to P. Consequently, an absorbance increase is expected in the depletion signal (due to the increase in the concentration of P). Likewise an absorbance decrease is expected at 350 nm (due to the decrease in the concentration of the bleached form which also absorbs at 350 nm) and a corresponding contribution in the proton release signal since the chromophore deprotonates in the P_{bl} to P transition. We already observed the latter two manifestations of this relaxation with the E46A mutant at pH = 8.3, i.e., near the pK_a of 7.9 (see ref *17*, Figures 1C and 2C). Here we observe these kinetic effects with E46Q, demonstrating that the apparent pK_a values for E46Q and E46A exactly match those of the P to P_{bl} dark equilibrium and provide a consistent explanation for all observations.

pH-Jump Stopped-Flow Kinetics of the P/P_{bl} Relaxation in the Dark. As a further test for the correctness of this interpretation, we carried out stopped-flow experiments to measure directly the relaxation kinetics between P and P_{bl} after a pH jump in the dark. Since the time resolution of our stopped-flow setup is about 2 ms and the expected kinetic time constant is about 10−15 ms at room temperature, these measurements were performed at about 10 °C in order to slow the kinetics and better resolve the absorbance change. The absorption spectra of E46Q at 2 ms, 300 ms, and 40 s after the pH jump from 6.3 to 4.8 are shown in Figure 8A. The time traces for the relaxation kinetics at 458 and 353 nm are shown in Figure 8B. With our CCD detection system, we recorded the time evolution over the entire spectral range from 300 to 780 nm. Analysis of this complete data set by SVD led to an exponential time constant of 28 ms in the time range below 400 ms. This time is marked in Figure 8B by the dashed vertical line. We also measured the time trace for the depletion signal after flash excitation at pH 4.8 and 10 °C (Figure 8C). Fitting of this time trace also led to a time constant of about 28 ms (dashed vertical line in Figure 8C). We conclude that these two time constants are equal.

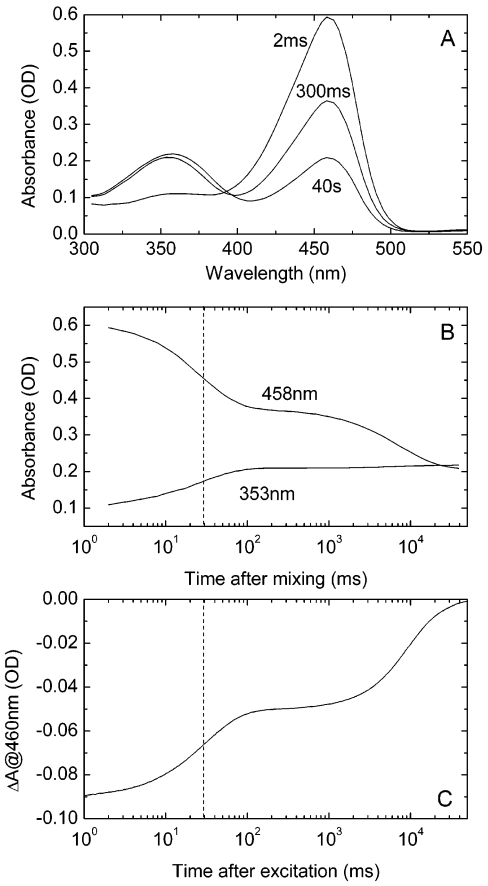

FIGURE 8: Stopped-flow relaxation kinetics of the P/P_{bl} equilibrium in the mutant E46Q after a pH jump from 6.3 to 4.8. The data are averages over 16 shots. (A) Absorption spectra 2 ms, 300 ms, and 40 s after mixing. (B) Kinetics of the transient absorption changes at 353 and 458 nm after the pH jump in the dark. (C) Kinetics of the transient absorption change at 460 nm during the photocycle for the same sample as in (A) and (B) after a pH jump (pH 4.8). The vertical line in (B) and (C) marks the common time constant of 28 ms. Conditions: 50 mM KCl, 10 °C, protein concentration after pH jump 13 μM.

This is direct evidence that our proposal that the 10 ms signal in the photocycle at 20 °C is due to the P/P_{bl} relaxation is correct. The slow time dependence in both traces of Figure 8B around 7 s is an artifact due to the formation of I_2 induced by the white measuring light and disappears when the light intensity is reduced. This effect from the measuring light is also evident in Figure 8A. Between 300 ms and 40 s the absorbance at 460 nm decreases further due to the formation of a photostationary state between P and I_2 in the white measuring beam (the spectrometer is between the sample and the CCD detector). The corresponding absorbance increase at 350 nm seems to be less than expected. This is again due to the relaxation effect between P and P_{bl}. As the amount of P decreases in the light at pH 4.8, some P_{bl} is transformed into P. This decrease in absorbance at 350 nm partially offsets the increase due to the formation of I_2.

DISCUSSION

Our results on the photocycle of the E46Q mutant of PYP, on the mechanism of chromophore protonation, and on the relaxation of the dark P/P_{bl} equilibrium will be discussed below using the scheme of Figure 9.

A major finding of this paper is that, in the mutant E46Q of PYP, no I_2 intermediate is formed at high pH (pK_a of

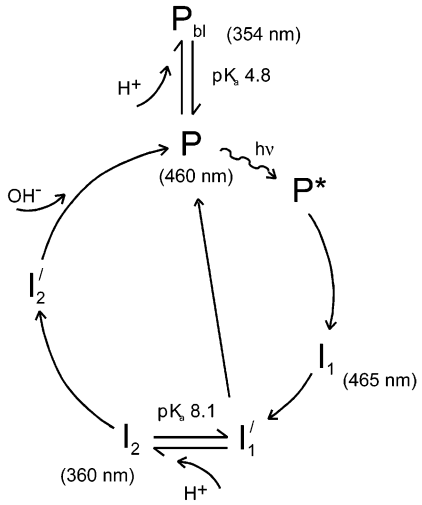

FIGURE 9: Proposed photocycle of the PYP mutant E46Q. The short-lived intermediates between P* and I_1 are left out since they are not relevant for the present work. The λ_{max} values of the intermediates were taken from our observations and are written next to each intermediate.

8.15). The most direct evidence for this conclusion stems from the pH dependence of the absorbance change at 370 nm, the wavelength characteristic for I_2 (Figures 1, 2B, and 3A). The titration of this amplitude provided a pK_a of 8.15 (Figure 3A). Supporting evidence was obtained from the pH dependence of the depletion signal which contains a contribution from the I_1 to I_2 transition with a rise time of about 50 μs (Figures 2A and 3A). The amplitude of this absorbance change also vanishes with a pK_a of 8.15 (Figure 3A). These data support the model shown in eq 1 and Figure 9 with a pH-independent reorientation of the chromophore which exposes its phenolate group to the protein surface in the transition from I_1 to I_1'. This is followed by rapid proton uptake by the chromophore in a pH-dependent equilibrium between I_1' and I_2. From Figure 1B, it is evident that, above this pK_a, I_1 or I_1' decays directly to P and that no intermediate with a protonated chromophore (I_2) is formed.

Equation 2 predicts that, well above pH 8.15, I_1' decays directly to P without proton uptake. Direct evidence for this branching was obtained from transient absorption measurements with the pH indicator dye cresol red (pK_a = 8.2) at pH 8.3. At this pH, somewhat above the pK_a of the I_1'/I_2 equilibrium, our model predicts that the majority of the molecules cycling will bypass I_2 and not take up a proton. The data of Figure 4A,B show that, at pH 8.3, proton uptake still occurs and remains perfectly synchronized with the rise of I_2, i.e., the protonation of the chromophore. The proton stoichiometry calculated from the dye signal is, however, reduced with respect to that at pH 6.3 where almost no branching occurs. With the stoichiometry defined as protons per PYP molecule cycling (I_1), the result from Figure 4C would be around 0.4. When the stoichiometry is defined, however, as protons taken up per I_2 molecule formed, the result is still close to 1. This is exactly as expected from branching: those few molecules returning to P via I_2 still transiently pick up one proton; the majority bypass I_2 without proton uptake.

A remarkably strong pH dependence was observed in the rate constant for the return from I_2 to the ground state between pH 4 and pH 8 (Figures 2, 3B, and 6). Similar observations were already reported in previous work (*7*), but we extended these measurements to lower pH, analyzed the data in a novel way, provided for the first time a consistent mechanistic interpretation involving OH^- uptake rather than H^+ release, and explained the pK_a of 8.1 as the pK_a of the exposed chromophore in the transient I_1' intermediate. Whereas in ref *7* the rate of this transition was plotted versus pH, here we plotted the logarithm of the rate constant versus pH. In this way we demonstrated the previously unrecognized fact that log *k* is exactly proportional to the pH with a slope of +1 over almost four pH units, implying that in this pH range *k* is first order in [OH^-]. This is direct evidence that the deprotonation of the chromophore is brought about by OH^- uptake from the aqueous medium. In the previous analysis (*7*), a Henderson−Hasselbalch equation was used, which is appropriate for a titration amplitude but not necessarily for a rate constant. Moreover, the linear scale for the rate constant led to an accumulation near zero of all the points below pH 7, thus preventing the recognition of the true nature of the pH dependence. The rate constants in Figure 3B simply do not obey the Henderson−Hasselbalch equation. Above pH 8.5, the rate constants were pH-independent (Figure 3B). These data were modeled on the basis of eq 2, which provided a complete description of the observations. From pH 4 to pH 8 the log of the rate constant increases linearly (Figure 3B) due to the corresponding increase in the concentration of free OH^-. Above pH 9, no I_2 is formed, no OH^- has to be taken up, and I_1' decays directly to P in a pH-independent manner. The fit of the pH dependence in Figure 3B with pK_a = 8.18 provided a second estimate of the chromophore pK_a in I_1', confirming our first determination.

We carried out analogous measurements on the pH dependence of the rate of return of P in the mutant E46A from pH 7.34 to pH 10.33 (Figure 7A). Again, a clear slowing occurred with decreasing pH. Analysis of these data showed that over the entire pH range these data also obeyed eq 3 with fit parameters pK_a = 8.75 and k_{app}^{∞} = 1.18 s^{-1} (fit not shown). For this mutant the experimentally accessible pH range was limited on the lower side by the fact that, well below the pK_a of 7.9, no P remains. These observations indicate that the mechanism of chromophore deprotonation by hydroxyl uptake as well as the pK_a of the I_1'/I_2 equilibrium are quite similar in E46Q and E46A. The pK_a of 8.75 is close to that of E46Q and appropriate for the phenolate of an exposed chromophore (see next section).

We interpreted the pK_a of 8.15 as the pK_a of the chromophore protonation in the transient I_1' intermediate in which the chromophore is exposed to the aqueous medium. This value is quite reasonable for a *p*-hydroxycinnamic group in water [pK_a of approximately 9 (*32*)].

Our value of 8.15 for the transient pK_a of E46Q in I_1' is much higher than the pK_a of 4.8 for the dark equilibrium between the yellow P form (460 nm) and the bleached P_{bl} form (354 nm). This equilibrium also involves chromophore protonation, however in an entirely different structure than in I_1', with a buried chromophore in a hydrophobic environment. The electronic energy levels of the chromophore are sensitive to this difference, leading to slightly different λ_{max} values for the protonated chromophore of E46Q: 360 nm in I_2 (Borucki et al., unpublished results) and 355 nm (*33*)/

354 nm (Borucki et al., unpublished results) in P_{bl}. In the absence of high-resolution structural information on the I_2 and P_{bl} states of this mutant, attempts to interpret these pK_a and λ_{max} values are highly speculative. Some insight might be gained, however, by comparison with the corresponding values for E46A and wild type. For E46A the pK_a's for the I_1'/I_2 and P/P_{bl} equilibria are 8.8 and 7.9, respectively, and the λ_{max} values are 465 nm (*27*)/469 nm (*42*), 361 nm (Borucki, unpublished results), and 352 nm (Borucki, unpublished results) for P, I_2, and P_{bl}, respectively. For wild type the pK_a's for I_1' and P_{bl} are >11 and 2.8, respectively, and the λ_{max} values are 446 nm, 360 nm (Borucki et al., unpublished results), and 350 nm (*25*, *26*) for P, I_2, and P_{bl}, respectively. In each protein species we expect the chromophore to be in a different environment (amino acids in binding pocket, hydrogen bonding, electrostatic interactions, dielectric constant) in P/P_{bl} and in I_1'/I_2. Therefore, no link or correlation is expected to exist between the pK_a's for the dark and photocycle equilibria. Looking at the numbers we note that the gap between these two pK_a's narrows in the sequence wild type (2.8 to >11), E46Q (4.8−8.1), and E46A (7.9−8.8). A meaningful comparison is prevented, however, by the fact that the pK_a of 2.8 for wild type refers to acid denaturation, which induces the chromophore deprotonation (*33*), whereas for E46Q and E46A the pK_a's refer to chromophore protonation in the folded proteins. This increase in the dark pK_a's seems to be correlated with the increase in λ_{max} (446, 460/462, 465/469 nm) and may be related to the weakening of the chromophore hydrogen bonds in the sequence wild type, E46Q, E46A, as has been pointed out already (*7*, *42*). The very similar pK_a's for the I_1'/I_2 equilibria in E46Q and E46A of 8.1 and 8.8 suggest that in both mutants protons are taken up by the surface-exposed chromophore in the I_1' to I_2 transition. The much higher value of >11 in wild type is intriguing and may be related to the pK_a of E46 (see discussion below). We obtained values of 360, 360, and 361 nm for the λ_{max} values of I_2 in wild type, E46Q, and E46A, respectively, from photostationary and transient absorption measurements. These results suggest that the local environment of the chromophore in I_2 is very similar in all three systems and support the idea that in each case the chromophore phenolate is solvent exposed in I_2. In ref *24* it was reported, however, that the λ_{max} value of 368 nm for I_2 in E46Q is red shifted with respect to wild type where a value of 357 nm was obtained. We were unable to reproduce the results. Moreover, the conclusion drawn from this observation, which implies that Q46 interacts with the chromophore in I_2 (*24*), is questionable and by no means unique. At least two I_2 species have been detected. I_2 and I_2' have substantially different structures (*13*, *16*). Moreover, it has been reported that λ_{max} for I_2' in wild type is red shifted with respect to I_2 (*36*). The question therefore arises to which state, I_2 or I_2', the λ_{max} value of 368 nm (*24*) refers. In view of the 2 ms time resolution in ref *24*, it seems most likely that it refers to I_2'. For our discussion the λ_{max} value in I_2 is the relevant one, however. Our data provide strong evidence that the chromophore is no longer in the binding pocket in I_2 and is instead protonated and deprotonated at the surface. Alternative explanations for the observations in ref *24* which make it consistent with our results on the site of the protonation reactions are (1) the 368 nm refers to the structurally altered state I_2' and (2) the red shift is due to exposure of the chromophore to the more polar environment at the protein surface. The data in ref *41* do not contradict explanation 2, since they were obtained in 6 M urea with a denatured protein.

At pH values near 4.8 the E46Q protein is presumably in the native structure with a buried chromophore. It was recently observed that this pK_a value increases in the presence of the chaotropic reagent potassium thiocyanate, which leads to unfolding of PYP (*33*). At 4 M KSCN a pK_a of about 7.3 was observed (*33*). Extrapolation to infinite KSCN concentration led to a limiting pK_a value of 8.1 (*33*). Since KSCN is a strong denaturant, this value of 8.1 was interpreted as the chromophore pK_a in the dark in a state in which it is almost completely exposed to solvent (*33*). The exact agreement with our value of 8.1 for the transient pK_a in I_1' is of course fortuitous. It is interesting, however, that the value obtained by denaturation and associated chromophore exposure in the dark state P is close to our value for the transient pK_a in the photocycle intermediate I_1' in which we claim that the chromophore is also exposed. This apparent "agreement" after unfolding of the P_{bl} form does not mean of course that any correlation exists between the pK_a values for the P/P_{bl} and I_1'/I_2 equilibria with different structures and interactions in the folded states.

The dramatic pH dependence of the time constant for the decay of the active state I_2 is similar to that observed for the decay of the M intermediate of bacteriorhodopsin (*31*), which may be considered to be the active state of this proton pump. The decay of M is pH-independent below pH 8, but above pH 8 log τ_M increases linearly with pH over four decades of time up to pH 12 (*31*). The pH dependence for the decay of M is almost the exact mirror image of what is observed here for PYP. Below pH 8, the deprotonated Schiff base of the chromophore is rapidly protonated in the decay of M by the internal proton donor D96 that is in turn rapidly reprotonated from the external medium. The intramolecular protonation from D96 is rate-limiting and pH-independent. At high pH, as protons became rare, the reprotonation of D96 from the solvent becomes rate-limiting and $k_M \sim [H^+]$ corresponding to $\tau_M \sim [H^+]^{-1}$. In bacteriorhodopsin, proton uptake becomes rate limiting at alkaline pH. In the case of the E46Q mutant of PYP, OH^- uptake from the external medium is rate limiting in the decay of I_2 below pH 8.1.

We have shown that the I_1' and I_2 intermediates are in a pH-dependent equilibrium, with a proton taken up from the aqueous medium and the chromophore being protonated in this transition. I_2 or I_2' is commonly regarded as the activated or signaling state of PYP, since in this long-living intermediate transient binding of the "response regulator" is presumed to occur (*1*). The model of eq 1 which was required to explain our results is thus similar to the pH-dependent equilibrium between the transient intermediate M_I (490 nm) and the signaling state M_{II} (380 nm) of rhodopsin (*34*). This transition also involves net proton uptake from the solvent as well as a protonation change of the chromophore. As for M_{II}, the I_2 state of PYP with protonated chromophore is also heterogeneous (I_2, I_2').

Another result of our investigation concerns the millisecond component in the photocycle signals for the decay of I_2 in E46Q and E46A. This effect was first observed in the depletion signal of E46A at pH 8.3 and interpreted as a fast component in the decay of I_2 (*27*). Similar millisecond

components were later also observed in the 370 nm signal (I_2) and the proton release kinetics for E46A at pH 8.3 (*17*). Again, these contributions were attributed to transitions between photocycle intermediates. Here we detected similar components for E46Q, found that the previous explanation is incorrect, and provided a very straightforward interpretation in terms of the dark equilibrium between the yellow form and the bleached form (P_{bl}) with protonated chromophore. The 10 ns laser flash depletes the yellow ground state P (see Figure 9). If the return to P via the photocycle is slower than the relaxation time of the P/P_{bl} equilibrium and the pH is close to the dark pK_a values of E46Q and E46A, the P/P_{bl} equilibrium will relax toward P before conclusion of the photocycle. This will lead to absorbance changes at 460 and 370 nm of the amplitude and signs observed, as well as corresponding contributions in the pH dye signal. Titrations of the amplitudes of the millisecond absorbance changes led to pK_a's of 4.8 for E46Q (Figure 6B) and 7.9 for E46A (Figure 7B). The good agreement of these pK_a values with those obtained by spectrophotometric titrations for the dark equilibrium is strong evidence for of our interpretation. Direct kinetic evidence was obtained from stopped-flow experiments in which the pH was rapidly changed from 6.3 to 4.8. At 10 °C, the time constant for the dark equilibrium between P and P_{bl} of 28 ms is the same as that observed in the photocycle under the same conditions (Figure 8B,C). This experiment proves that the millisecond component in the photocycle signal is indeed due to the relaxation of the P/P_{bl} equilibrium after perturbation by the flash excitation. The temperature was reduced to 10 °C to better resolve the stopped-flow signal. In pH-jump stopped-flow experiments with wild type around pH 2.8 relaxation times of about 10 ms were observed at 5 °C, i.e., in the same time range as our results with E46Q (*35*). These wild-type results, however, contain contributions from unfolding reactions that induce the chromophore protonation. An advantage of E46Q and in particular E46A is that, because of the high pK_a values for the P/P_{bl} transition, the proton relaxation kinetics can be studied without the complications from the folding reactions.

Our results show conclusively that, in the mutant E46Q, the chromophore is transiently protonated from the aqueous medium in I_2. In the return from I_2 to the initial state deprotonation occurs by OH^- uptake from the aqueous medium. Similar observations were made for E46A. Moreover, the formation of the I_2 intermediate is faster in E46Q than in wild type and perfectly synchronized with the uptake of protons from the aqueous medium (*17*). These findings show that E46 is not required for the formation of I_2. In wild type and in the yellow form of the mutant E46A, the kinetics of chromophore protonation and proton uptake are also tightly coupled (*17*), and we have argued on this basis that, in these systems, the chromophore is also protonated via the solvent. Here, we have uncovered further details of this mechanism in E46Q, namely, the pH-dependent equilibrium between I_1' and I_2 and the chromophore deprotonation by hydroxyl uptake. Whether these features of the mechanism of chromophore protonation are also operative in wild type remains to be seen, but there are a number of indications that point in this direction.

First, we observed in wild type above pH 9.0 that the ratio of the amplitudes of the absorbance changes at 370 and 490 nm decreases with increasing pH (Figure 5). Moreover, the absorbance change at 490 nm due to I_1 remains positive after the rise of I_2. These data (Figure 5B) clearly show that, at pH 10.94, I_1 and I_2 are in equilibrium and decay together in the recovery of P. These observations suggest that the photocycle of wild type changes above pH 10 in a similar way as that of E46Q near the pK of 8.15; that is, less I_2 is formed and some I_1 decays directly to P. The conclusions reached about the mechanism of chromophore protonation/deprotonation in E46Q thus may apply at least in part to wild type. Due to irreversible effects above pH 11, data could only be collected below this pH. However, we can conclude that, qualitatively, the kinetic features in the alkaline region are similar in wild type and E46Q and that the pK_a of the I_1'/I_2 equilibrium is above 11 in wild type. The observation that the pK_a of the chromophore equilibrium in I_1'/I_2 is shifted from 8.15 in E46Q to above 11 in wild type suggests that the chromophore is less exposed or more strongly hydrogen-bonded in I_1' in wild type than in E46Q. Like the corresponding shift in the chromophore pK_a in the dark, this shift suggests that wild type has a "tighter" structure than the E46 mutants. We call attention to the fact that this comparison between the pK_a's of the E46 mutants and wild type is complicated by the ionization of E46 in wild type which is estimated to occur between pH 10 and 12 (*33*). In the alkaline form of wild-type PYP, above this pK_a, the λ_{max} value is blue shifted (*33*). This second protonation equilibrium (of E46) in the same pH range complicates the discussion. We note that a red-shifted form of I_2 was reported for wild type at alkaline pH (*36*, *40*). A species with an absorption maximum at 420 nm was detected in steady-state light/dark difference spectra which formed with a pK_a >10 (*40*). A species with λ_{max} around 430 nm was observed in the transient spectra for the ground state recovery and developed with a pK_a of 10 (*36*). Both were attributed to an I_2 form with deprotonated chromophore. It is conceivable that this "alkaline pB" is related to our I_1' species, which we detected in time-resolved experiments (Figure 5B), although our I_1' is red shifted with respect to P and although our estimate for the pK_a is above 11.

Second, further support for a similar mechanism of chromophore protonation/deprotonation in E46Q and wild-type comes from recent kinetic isotope experiments with wild type (*36*). Here it was reported that the rate constant for the decay of I_2 in wild type displays a reverse kinetic isotope effect; i.e., the rate is faster in D_2O than in H_2O (*36*). From this observation, and the fact that OD is a stronger base than OH, it was concluded that in this transition the chromophore deprotonates by hydroxyl uptake (*36*). No direct comparison was shown between kinetic traces in H_2O and D_2O, making it difficult to judge whether a reverse kinetic isotope effect does in fact occur. Nevertheless, the conclusion that I_2 decays by OH^- uptake agrees with our direct experimental proof of this mechanism in the E46Q mutant ($k \sim [OH^-]$, Figure 3B). The mechanism of chromophore deprotonation thus seems to be similar in E46Q and wild type and involves in both cases chromophore protonation/deprotonation reactions near the protein surface by exchange with the aqueous medium, as we have previously argued (*17*, *27*, *37*).

REFERENCES

1. Cusanovich, M. A., and Meyer, T. (2003) *Biochemistry 42*, 4759−4770.
2. Hellingwerf, K. J., Hendriks, J., and Gensch, T. (2003) *J. Phys. Chem. A 107*, 1082−1094.
3. Pellequer, J.-L., Wager-Smith, K. A., Kay, S. A., and Getzoff, E. D. (1998) *Proc. Natl. Acad. Sci. U.S.A. 95*, 5884−5890.
4. Taylor, B. L., and Zhulin, I. B. (1999) *Microbiol. Mol. Biol. Rev. 63*, 479−506.
5. Kim, M., Mathies, R. A., Hoff, W. D., and Hellingwerf, K. J. (1995) *Biochemistry 34*, 12669−12672.
6. Borgstahl, G. E. O., Williams, D. R., and Getzoff, E. D. (1995) *Biochemistry 34*, 6278−6287.
7. Genick, U. K., Devanathan, S., Meyer, T. E., Canestrelli, I. L., Williams, E., Cusanovich, M. A., Tollin, G., and Getzoff, E. D. (1997) *Biochemistry 36*, 8−14.
8. Kort, R., Vonk, H., Hoff, W. D., Crielaard, W., and Hellingwerf, K. J. (1996) *FEBS Lett. 382*, 73−78.
9. Unno, M., Kumauchi, M., Sasaki, J., Tokunaga, F., and Yamauchi, S. (2000) *J. Am. Chem. Soc. 122*, 4233−4234.
10. Meyer, T. E., Yakali, E., Cusanovich, M. A., and Tollin, G. (1987) *Biochemistry 26*, 418−423.
11. Hoff, W. D., Van Stokkum, I. H. M., Van Ramesdonk, H. J., Van Brederode, M. E., Brouwer, A. M., Fitch, J. C., Meyer, T. E., Van Grondelle, R., and Hellingwerf, K. J. (1994) *Biophys. J. 67*, 1691−1705.
12. Genick, U. K., Soltis, S. M., Kuhn, P., Canestrelli, I. L., and Getzoff, E. D. (1998) *Nature 392*, 206−209.
13. Brudler, R., Rammelsberg, R., Woo, T. T., Getzoff, E. D., and Gerwert, K. (2001) *Nat. Struct. Biol. 8*, 265−270.
14. Genick, U. K., Borgstahl, G. E. O., Ng, K., Ren, Z., Pradewand, C., Burke, P. M., Srajer, V., Teng, T. Y., Schildkamp, W., McRee, D. E., Moffat, K., and Getzoff, E. D. (1997) *Science 275*, 1471−1475.
15. Imamoto, Y., Mihara, K., Hisatomi, O., Kataoka, M., Tokunaga, F., Bojkova, N., and Yoshihara, K. (1997) *J. Biol. Chem. 272*, 12905−12908.
16. Xie, A., Kelemen, L., Hendriks, J., White, B. J., Hellingwerf, K. J., and Hoff, W. D. (2001) *Biochemistry 40*, 1510−1517.
17. Borucki, B., Devanathan, S., Otto, H., Cusanovich, M. A., Tollin, G., and Heyn, M. P. (2002) *Biochemistry 41*, 10026−10037.
18. Hendriks, J., Gensch, T., Hviid, L., van der Horst, M. A., Hellingwerf, K. J., and van Thor, J. J. (2002) *Biophys. J. 82*, 1632−1643.
19. Rubinstenn, G., Vuister, G. W., Mulder, F. A. A., Düx, P. E., Boelens, R., Hellingwerf, K. J., and Kaptein, R. (1998) *Nat. Struct. Biol. 5*, 568−570.
20. Sasaki, J., Kumauchi, M., Hamada, N., Oka, T., and Tokunaga, F. (2002) *Biochemistry 41*, 1915−1922.
21. Imamoto, Y., Kamikubo, H., Harigai, M., Shimizu, N., and Kataoka, M. (2002) *Biochemistry 41*, 13595−13601.
22. Lee, B.-C., Croonquist, P. A., Sosnick, T. R., and Hoff, W. D. (2001) *J. Biol. Chem. 276*, 20821−20823.
23. Van Brederode, M. E., Hoff, W. D., Van Stokkum, I. H. M., Groot, M.-L., and Hellingwerf, K. J. (1996) *Biophys. J. 71*, 365−380.
24. Imamoto, Y., Mihara, K., Tokunaga, F., and Kataoka, M. (2001) *Biochemistry 40*, 14336−14343.
25. Meyer, T. E. (1985) *Biochim. Biophys. Acta 803*, 175−183.
26. Hoff, W. D., van Stokkum, I. H. M., Gural, J., and Hellingwerf, K. J. (1997) *Biochim. Biophys. Acta 1322*, 151−162.
27. Devanathan, S., Brudler, R., Hessling, B., Woo, T. T., Gerwert, K., Getzoff, E. D., Cusanovich, M. A., and Tollin, G. (1999) *Biochemistry 38*, 13766−13772.
28. Borucki, B., Otto, H., and Heyn, M. P. (1999) *J. Phys. Chem. B 103*, 6371−6383.
29. Otto, H., Marti, T., Holz, M., Mogi, T., Stern, L. J., Engel, F., Khorana, H. G., and Heyn, M. P. (1990) *Proc. Natl. Acad. Sci. U.S.A. 87*, 1018−1022.
30. Van Thor, J., Borucki, B., Crielaard, W., Otto, H., Lamparter, T., Hughes, J., Hellingwerf, K. J., and Heyn, M. P. (2001) *Biochemistry 40*, 11460−11471.
31. Otto, H., Marti, T., Holz, M., Mogi, T., Lindau, M., Khorana, H. G., and Heyn, M. P. (1989) *Proc. Natl. Acad. Sci. U.S.A. 86*, 9228−9232.
32. Kroon, A. R., Hoff, W. D., Fennema, H. P. M., Gijzen, J., Koomen, G.-J., Verhoeven, J. W., Crielaard, W., and Hellingwerf, K. J. (1996) *J. Biol. Chem. 271*, 31949−31956.
33. Meyer, T. E., Devanathan, S., Woo, T. T., Getzoff, E. D., Tollin, G., and Cusanovich, M. A. (2003) *Biochemistry 42*, 3319−3325.
34. Dickopf, S., Mielke, T., and Heyn, M. P. (1998) *Biochemistry 37*, 16888−16897.
35. Lee, B.-C., Croonquist, P. A., and Hoff, W. D. (2001) *J. Biol. Chem. 276*, 44481−44487.
36. Hendriks, J., van Stokkum, I. H. M., and Hellingwerf, K. J. (2003) *Biophys. J. 84*, 1180−1191.
37. Meyer, T. E., Cusanovich, M. A., and Tollin, G. (1993) *Arch. Biochem. Biophys. 306*, 515−517.
38. Laidler, K. J. (1987) *Chemical Kinetics*, 3rd ed., Harper Collins, New York.
39. Fersht, A. (1999) *Structure and Mechanism in Protein Science*, Freeman, New York.
40. Hendriks, J., Hoff, W. D., Crielaard, W., and Hellingwerf, K. J. (1999) *J. Biol. Chem. 274*, 17655−17660.
41. Ohishi, S., Shimizu, N., Mihara, K., Imamoto, Y., and Kataoka, M. (2001) *Biochemistry 40*, 2854−2859.
42. Imamoto, Y., Koshimizu, H., Mihara, K., Hisatomi, O., Mizukami, T., Tsujimoto, K., Kataoka, M., and Tokunaga, F. (2001) *Biochemistry 40*, 4679−4685.

BI034315D